1

2

3

4

5

6

7 **Interactions between silver nanoparticles/silver ions and liposomes: evaluation of the**
8 **potential passive diffusion of silver and effects of speciation**

9

10

11

12

13

14 CAMILLE GUILLEUX, PETER G.C. CAMPBELL and CLAUDE FORTIN*

15

16

17 Institut national de la Recherche scientifique, INRS Eau Terre et Environnement

18 490 rue de la Couronne

19 Québec, Canada G1K 9A9

20

21

22

23

24 *Corresponding author
25 Email claude.fortin@ete.inrs.ca; Telephone (418) 654-3770

26   **Abstract**

27   Silver nanoparticles, used mainly for their antibacterial properties, are among the most common

28   manufactured nanomaterials. How they interact with aquatic organisms, especially how they cross

29   biological membranes, remains uncertain. Free Ag^+ ions, released from these nanoparticles, are

30   known to play an important role in their overall bioavailability. In this project, we have studied

31   the uptake of dissolved and nanoparticulate silver by liposomes. These unilamellar vesicles,

32   composed of phospholipids, have long been used as models for natural biological membranes,

33   notably to study the potential uptake of solutes by passive diffusion through the phospholipid

34   bilayer. The liposomes were synthesized using extrusion techniques and were exposed over time

35   to dissolved silver under different conditions where Ag^+, $AgS_2O_3^-$ or $AgCl^0$ were the dominant

36   species. Similar experiments were conducted with the complexes $HgCl_2^0$ and $Cd(DDC)_2^0$, both of

37   which are hydrophobic and known to diffuse passively through biological membranes. The

38   uptake kinetics of Ag^+, $HgCl_2^0$ and $Cd(DDC)_2^0$ show no increase in internalized concentrations

39   over time, unlike $AgS_2O_3^-$ and $AgCl^0$, which appear to pass through the phospholipid bilayer.

40   These results are in contradiction with our initial hypothesis that lipophilic Hg and Cd complexes

41   would be able to cross the membrane whereas silver would not. Encapsulated tritiated water

42   inside the liposomes was shown to rapidly diffuse through the lipid bilayer, suggesting a high

43   permeability. We hypothesize that monovalent anions or complexes as well as small neutral

44   complexes with a strong negative dipole can diffuse through our model membrane. Finally,

45   liposomes were exposed to 5-nm polyvinylpyrrolidone-coated silver nanoparticles over time. No

46   significant uptake of nanoparticulate silver was observed. Neither disruption of the membrane nor

47   invagination of nanoparticles into the liposomes was observed. This suggests that the main risk

48   caused by AgNPs for non-endocytotic biological cells would be the elevation of the free silver

49   concentration near the membrane surface due to adsorption of AgNPs and subsequent

50   oxidation/dissolution.

51   Keywords: model membrane, liposome, metals, speciation, silver nanoparticles, passive diffusion.

52

53

Introduction

54

55 The free metal ion is normally the most chemically reactive form for many cationic trace metals

56 in the environment and it is recognized as the best predictor of their uptake and toxicity

57 (Campbell 1995). This relation between the free metal ion activity and metal uptake reflects the

58 dominant mode of transmembrane transport for cationic trace metals, namely facilitated transport

59 involving membrane-bound transporters or channels (Campbell 1995). However, one should also

60 take a close look at small and hydrophobic complexes of trace metals that are present in natural

61 waters, as they may bypass the normal membrane transport systems and enter biological cells by

62 simple passive diffusion across the lipid bilayer (Phinney and Bruland 1994). Turner and Mawji

63 (2004) reviewed the literature in this area and summarized the experimentally determined

64 octanol-water partition coefficients (K_{ow}) for neutral Al, Cu, Mn and Pb complexes (from 0.0003

65 for Al-citrate to 10,000 for Pb-diethyl-dithiocarbamate ($Pb(DDC)_2^0$)). They compared the

66 coefficients they determined for five natural waters with the literature and concluded that such

67 hydrophobic complexes are present in natural surface waters.

68 The involvement of neutral complexes in transmembrane transport is somewhat controversial,

69 notably for $AgCl^0$. Reinfelder and Chang (1999) suggested that the $AgCl^0$ complex could pass

70 through the cell membrane of the euryhaline marine microalga *Thalassiosira weissflogii* by

71 passive diffusion. They experimentally determined the octanol-water partition coefficients (K_{ow})

72 at increasing chloride concentrations to estimate the contribution of each silver chloride complex

73 and showed that $AgCl^0$ had the highest value (K_{ow} = 0.09), suggesting that $AgCl^0$ could diffuse

74 through the algae phospholipid bilayer more easily than other silver species. This K_{ow}, however,

75 is much lower than that of $HgCl_2^0$ (3.3, Mason et al. (1996)) and of $Cd(DDC)_2^0$ (270 ± 28,

76 Boullemant et al. (2009)), the internalisation of which have been shown to occur via passive

77 diffusion. In contrast, Fortin and Campbell (2000) studied silver uptake by the freshwater green

78 alga *Chlamydomonas reinhardtii* and argued against the $AgCl^0$ passive diffusion hypothesis. For

79 example, they found that silver uptake was only slightly affected when the total silver

80 concentration was fixed and the relative importance of the $AgCl^0$ complex was varied by

81 adjusting the chloride concentration.

82 Silver nanoparticles are being increasingly used and contribute to the overall mobility of silver in

83 the environment. Blaser et al. (2008) and Gottschalk et al. (2009) estimated, using theoretical

84 models based on projected use of silver nanoparticles, that nanosilver concentrations could reach

85 40-320 ng/L in European rivers and 0.09-0.43 ng/L in American surface waters. Although silver

86 nanoparticles will likely dissolve or react with suspended particles (Blaser et al. 2008), they could

87   also come into contact with aquatic organisms. However, the assimilation mechanisms of

88   nanoparticles are not well known yet (Treuel et al. 2013). Additionally, their transformations and

89   the speciation of the resulting species will directly affect their bioavailability and toxicity towards

90   aquatic organisms (Levard et al. 2012). To our knowledge, there is only one report of intact

91   nanoparticle assimilation by a unicellular organism (Miao et al. 2010). In this paper, the authors

92   suggested that silver nanoparticles were taken up by phagocytosis, but passive uptake of silver

93   nanoparticles through cell membranes could also contribute to the overall internalization.

94   Phospholipid membranes and especially liposomes, as presented in Figure 1a, have often been

95   used as abiotic models of biological membranes, especially for pharmacological research. Indeed,

96   many of the properties of these vesicles, such as osmotic swelling and permeability to small

97   solutes, are similar to those of natural membranes (Sessa and Weissmann 1968). Rusciano et al.

98   (2009) examined, for example, the interaction between nano-sized organic carbon particles and

99   liposomes. Moghadam et al. (2012) used liposomes to study the influence of the concentration

100   and coating of gold and titanium dioxide nanoparticles on membrane disruption.. The aims of the

101   present study were to determine if liposomes can be used as a model to study the passive

102   diffusion of Ag(I) and the interactions between 5-nm PVP-coated AgNPs and the lipid bilayer.

103   Large unilamellar vesicles made of egg phosphatidylcholine (PC) were prepared. PC is one of the

104   main phospholipids in natural membranes, especially in aquatic invertebrates and algae. One of

105   the objectives of this approach was to explore whether or not silver nanoparticles can cross the

106   cell membrane of small unicellular organisms such as algae. The PC gel-liquid crystalline

107   transition temperature ($-2.5°C$) is low enough to allow us to work at ambient temperature

108   (Koynova and Caffrey 1998). The simplicity of the membrane composition was important so that

109   only passive diffusion through the lipid bilayer could be considered. Similar experiments were

110   performed with $HgCl_2^0$ and $Cd(DDC)_2^0$, known to be sufficiently hydrophobic to pass through the

111   biological membranes as mentioned previously, and tritiated water to evaluate the suitability or

112   the potential limits of our model membrane.

Materials and methods

Buffer preparation

115   All plasticware was soaked for 24 h in 10% HNO_3 (v/v), rinsed three times with deionized water

116   and three times with ultrapure water ($\geq$ 18 MΩ cm) prior to use. Phenol red and sodium

117   thiosulfate pentahydrate were obtained from Fisher Scientific. The 2-(N-morpholino)-

118   ethanesulfonic acid (MES) and 2-(N-morpholino-propanesulfonic acid (MOPS) were obtained

4

119   from Sigma-Aldrich. Table 1 shows the composition of the different buffer solutions used in this

120   study. The buffers were prepared by using stock solutions (0.1 M) of each of the components,

121   which had been previously filtered through 0.2 µm polycarbonate filter membranes. The pH of

122   the buffer solutions was adjusted using a 1 M NaOH solution and the ionic strength was fixed at

123   25 meq/L by addition of KNO_3; the pH was chosen to be environmentally relevant, based on the

124   average pH of freshwater (6.3-8.3, MDDELCC (2016)) and internal cell medium (5.5-7.5,

125   Carrozzino and Khaledi (2005))**.** In order to maintain the concentration gradient between the

126   exposure solution and the internal solution trapped in the liposomes, a strong ligand was added to

127   the liposomes' inner solution. We chose thiosulfate because it forms very stable hydrophilic

128   complexes with silver ($AgS_2O_3^-$, $Ag(S_2O_3)_2^{3-}$: log K_1 = 8.82, log β_2 = 13.50, Martell et al. (2004))

129   and mercury ($Hg(S_2O_3)_2^{2-}$, $Hg(S_2O_3)_3^{4-}$: log K_1 = 29.27, log K_2 = 30.8, Nyman and Salazar

130   (1961)). For cadmium, ethylenediaminetetraacetic acid (EDTA) was chosen as the internal ligand

131   ($Cd(EDTA)^{2+}$, log K = 18.1, Martell et al. (2004)). The ionic strength and species distribution in

132   each solution were calculated using MINEQL+ chemical equilibrium software (v.4.6; Schecher

133   and McAvoy (2001)). According to these calculations, silver and mercury were mostly (>99%)

134   bound to thiosulfate when placed in the internal buffer solution, for all tested conditions;

135   similarly, cadmium speciation in the internal buffer solution was dominated by its complex with

136   EDTA (>99%).

137   Liposomes synthesis

138   Egg yolk phosphatidylcholine (EPC) was provided by Avanti Polar Lipids. Internally threaded

139   cryogenic vials (5 mL) were obtained from Fisher Scientific. Polycarbonate filters were provided

140   by Millipore. Liposomes were prepared by the extrusion technique (Ducat et al. 2010). Egg yolk

141   phosphatidylcholine was initially dissolved in a mixture of organic solvents (9:1;

142   chloroform:methanol), kept in the freezer at -20°C. The solvents were evaporated under a gentle

143   nitrogen flow (1 h at 35°C). The cryogenic vial was then placed in a desiccator under vacuum for

144   2 h to remove traces of solvent. The lipids were then re-suspended in the internal buffer solution

145   by using a vortex mixer. Multilamellar vesicles (or MLVs) are spontaneously formed under these

146   conditions (Berger et al. 2001). Eight freeze-thaw cycles were then applied in order to break the

147   phospholipid bilayers by the formation of ice crystals formed during the freezing step (Castile and

148   Taylor 1999) and form large unilamellar vesicles. Briefly, the vial was placed in a liquid nitrogen

149   bath for 1 min, then in a water bath at 45°C for 5 min and lastly shaken on a vortex mixer for 1

150   min. The vesicles were finally passed six times through an extruding system containing two

151   stacked 200-nm polycarbonate filters (Figure S1 in the supporting information (SI)) (Ducat et al.

152 2010). Two syringes were used alternately, without changing the filter orientation, to force the
153 liposomes through the filters, minimizing losses.

154 The mean diameter and size distribution of the liposomes were analyzed by dynamic light
155 scattering (DLS) using a Malvern Zetasizer Nano-ZS instrument. Malvern folded capillary zeta
156 cells were cleaned three times with ethanol and three times with ultrapure water before use for
157 measurements. Six measures were taken at 25°C for each preparation, each measure
158 corresponding to six scans of 15 s each.

159 Size-exclusion chromatography

160 The aim of this step was to transfer the liposomes to the pH 7.4 exposure buffer solution and to
161 verify the liposomes' membrane integrity. Indeed, if there were any leakage out of the liposomes,
162 the phenol red dye, yellow in the pH 6.0 internal buffer solution, would reach the pH 7.4 outer
163 solution and turn red. Sephadex G50 Fine resin was obtained from Fisher Scientific. The 2.5 x 50
164 cm Econo-Column Chromatography columns were purchased from Bio-Rad. The transfer was
165 done by passing the liposomes through a Sephadex G50 resin filled column, used for size-
166 exclusion chromatography (SEC) and previously equilibrated with the pH 7.4 exposure buffer
167 solution. The first colored fraction (yellow), containing the liposomes, was collected and analyzed
168 on a Varian Cary 50 UV-spectrophotometer at 432 nm (Agilent Technologies). Just after the
169 fraction collection and before using the large unilamellar vesicles (LUVs), the vials containing
170 the liposomes were kept on ice to avoid potential membrane damage. The mean diameter and size
171 distribution of the liposomes in the pH 7.4 exposure buffer solution were determined again as
172 mentioned above.

173 Total phosphorus analysis

174 In order to quantify the amount of liposomes used, a relationship between the absorbance of a
175 sample at 432 nm (phenol red absorbance wavelength) and its total phosphorus concentration (g
176 P/L) was determined. The total phosphorus concentration was determined by colorimetry. Briefly,
177 a sample aliquot was diluted in a 0.2 % sulfuric acid solution. After addition of 0.5 g of potassium
178 persulfate, the solution was autoclaved for 45 min between 83 and 103 kPa. A solution of 7.5 g/L
179 ammonium paramolybdate and 0.14 g/L potassium antimonyl tartrate in 8.8% H_2SO_4 was stirred
180 together with a solution of 25 g/L ascorbic acid. This mixture was added to the autoclaved
181 solution to form a blue complex with phosphate. A standard solution of KH_2PO_4 was used to
182 establish a calibration curve and a control sample initially containing 3.54 mg P/L was used to

183 verify the method accuracy. Absorbance measurements were made on a UV-spectrophotometer at

184 885 nm. The phosphorus calibration curve is given in Figure S2 (SI).

185 The total number of phosphatidylcholine molecules per chromatographic fraction, N_{PC}, could

186 then be calculated as follows:

187 $$n = C \times V = \frac{N_{PC}}{N_a} \tag{1}$$

188 $$\Rightarrow N_{PC} = C \times V \times N_a = \frac{x}{31} \times V \times N_a \tag{2}$$

189 where n = amount of PC (moles), C = concentration (moles PC/L), V = fraction volume (L),

190 N_a = Avogadro constant ($6.022 \cdot 10^{23}$ mole^{-1}), x = total phosphorus concentration in the fraction

191 (g P/L).

192 The total number of liposomes per chromatographic fraction is:

193 $$N_{LUV} = \frac{N_{PC}}{N_{tot}} \tag{3}$$

194 The total number of phosphatidylcholine molecules per liposome, N_{tot}, depends on the

195 liposome's diameter d (nm) (Enoch and Strittmatter 1979):

196 $$N_{tot} = 17.69 \times ((\frac{d}{2})^2 + (\frac{d}{2} - 5)^2) \tag{4}$$

197 Then, $$N_{LUV} = \frac{\frac{x}{31} \times V \times N_a}{17.69 \times ((\frac{d}{2})^2 + (\frac{d}{2} - 5)^2)} \tag{5}$$

198

199 Short term accumulation experiments

200 *Liposomes exposed to dissolved silver*

201 This preliminary experiment was done to quantify any contribution of the free silver ion, released

202 from the nanoparticles, to silver uptake by the liposomes. This was also useful to quantify the

203 potential contribution of free silver ions in the $AgS_2O_3^-$ and the $AgCl^0$ experiments (Table 2).

204 Radioactive ^{110m}Ag (as $AgNO_3$ in 0.1 M HNO_3, initial specific activity = 5.15 mCi/mL, total [Ag]

205 = 5 mM) was supplied by the Radioisotope Centre Polatom. Short-term (100 min) experiments

206 were performed at pH 7.40 ± 0.02 with an initial concentration of 30 nM ^{110m}Ag in the exposure

207   solution. As radioactive silver produces radiation at 657.76 keV, every analysis was done

208   between 580 and 1020 keV on a Wizard 2 automatic gamma counter (PerkinElmer), with a

209   counting time of 300 s and a maximal counting number of 100,000 events.

210   Radioactive silver was diluted in a pH 7.4 buffer solution with or without a silver-binding ligand

211   (thiosulfate or chloride), the pH was adjusted using a 1 M NaOH solution and the ionic strength

212   was fixed with KNO_3 to reach the same ionic strength as the internal buffer held within the

213   liposomes (Tables 1 and 2). The solutions were placed in three 125-mL HDPE vials. An aliquot

214   of each solution was then taken and analyzed on the gamma counter to determine the initial silver

215   exposure concentration. An aliquot of the liposomes suspension was then added to the exposure

216   solutions and the vials were placed on a Wrist Action Shaker (Burrell) for 100 min. The liposome

217   concentration was selected so that the external silver concentration did not decrease more than

218   10% during the exposure period. The thiosulfate concentration in the inner solution (1.33 mM)

219   was chosen to ensure that it was always greater than the internal silver concentration, so that a

220   free Ag^+ concentration gradient was maintained between the exposure solution and the solution

221   held within the liposomes.

222   In the time-course experiments, an aliquot from each vial was taken every 10 min and placed in a

223   15-mL vial containing Ambersep GT 74 resin (300 mg) (Sigma-Aldrich), a weakly acidic cation

224   exchange resin with very high affinity for soft metal ions such as mercury, silver and cadmium.

225   The vials were shaken for 5 min. After allowing the resin to settle, an aliquot of the supernatant

226   was taken and analyzed on the gamma counter (see Figure S3 in the supporting information for a

227   detailed illustration of the experimental design of these uptake experiments).

228   Similar experiments were conducted with liposomes prepared with an internal buffer solution

229   without thiosulfate (internal buffer solution (w/o trap) in Table 1) and the results were compared

230   to the previous ones. As only adsorption to the liposomes could occur in these experiments, it

231   allowed us to differentiate between uptake (C, D or E in Figure 1c) and adsorption (B in Figure

232   1c) by comparing the first two experiments: if the results are the same, only adsorption is

233   occurring. On the other hand, if there is a difference, one could conclude that silver can pass

234   through the liposome membrane.

235   *Liposomes exposed to $HgCl_2^0$*

236   Similar experiments were conducted in a medium where $HgCl_2^0$ was the dominant species

237   (exposure solution 4 in Table 2). Mercury was diluted in a pH 7.4 buffer solution with chloride as

238   the mercury ligand. The liposomes were exposed as explained previously for silver. Ambersep

239   GT 74 resin (500 mg) was then added to stop the exposure and bind non-adsorbed and non-

240   internalized mercury. Mercury was analysed by inductively coupled plasma – mass spectrometry

241   (ICP-MS, Model XSeries 2, Thermo Scientific). Briefly, samples were diluted in 10% HCl and

242   3% H_2O_2. Gold was also added to a concentration of 10 ppm to prevent any adsorption of Hg on

243   tube walls. Instrument response was calibrated within the expected range (0 to 28 nM) with

244   standard solutions obtained from PlasmaCAL SCP Science. An internal standard solution of [103]Rh

245   (58 nM) was used to correct analytical signal suppression (or enhancement) due to matrix effects

246   or signal fluctuations. Custom ICP Standards (SCP Science) were used as controls to verify the

247   precision and accuracy of the method (see Figure S3).

248   The mean diameter and size distribution of the liposomes exposed to mercury for 100 min were

249   analyzed once by dynamic light scattering (DLS) using a Malvern Zetasizer Nano-ZS instrument

250   to verify there was no change.

251   *Liposomes exposed to Cd(DDC)$_2^0$*

252   Radioactive Cd (as $CdCl_2$ in 0.5 M HCl, initial specific activity = 37.1 µCi/mL, total [Cd] = 1.0

253   µM) was supplied by Eckert & Ziegler). Similar experiments were conducted in a medium where

254   Cd(DDC)$_2^0$ was the dominant species (exposure solution 5 in Table 2). Cadmium was diluted in a

255   pH 7.4 buffer solution with sodium diethyl-dithiocarbamate (DDC) as the cadmium ligand. The

256   liposomes were exposed as explained before. As radioactive cadmium produces radiation at 22

257   keV, each analysis was done between 16 and 32 keV on a Wizard 2 automatic gamma counter

258   (PerkinElmer)), with a counting time of 600 s and a maximal counting number of 10,000,000

259   events (see Figure S3).

260   *Liposomes exposed to tritiated water*

261   The basic permeability of the phospholipid bilayer was determined by measuring the diffusion of

262   tritiated water from the internal to the external buffer. Tritiated water (initial specific activity = 10

263   mCi/mL) was supplied by DuPont. The liposomes were prepared in a buffer containing tritiated

264   water so as to encapsulate ^3H_2O inside the vesicles. The liposomes were then transferred to the

265   pH 7.4 exposure buffer solution suing the Sephadex column as described above. Fractions from

266   the column were collected every 10 or 20 mL and analysed on the liquid scintillation analyzer and

267   UV-visible spectrophotometer to quantify ^3H and P respectively. Each analysis was done between

268 0 and 18.6 keV using Ecolite scintillation cocktail (MP Biomedicals) on a Tri-Carb 2910TR

269 liquid scintillation analyzer (PerkinElmer), with a counting time of 1 min.

270 *Liposomes exposed to silver nanoparticles*

271 A solution of 5-nm PVP-coated silver nanoparticles with an initial concentration of 9 mM

272 (Nanocomposix, San Diego, CA) was used in these experiments. In order to be able to compare

273 the results for silver nanoparticles with those for dissolved silver, the concentration of free silver

274 in the exposure solution 6 should be equal to that in the exposure solution 1 (Table 2).

275 Ultracentrifugation was used to determine the free silver content in AgNPs solutions of different

276 concentrations, between 42 and 463 nM, prepared from the 9 mM solution. Silver nanoparticles

277 were diluted in a solution at pH 7.4 as shown in Table 2. Ultracentrifugation tubes (Amicon

278 Ultra-15, Millipore), equipped with filters with a molecular weight cut-off (MWCO) of 3 kDa,

279 were pre-rinsed with the external buffer solution in order to remove glycerin present on the

280 membranes. Filters were then pre-equilibrated with the AgNPs solutions by successive

281 centrifugations at 3700 x g for 20 min, as dissolved silver adsorbs on the membrane surface to a

282 non-negligible extent. After each centrifugation, total and ultrafiltered Ag concentrations were

283 analyzed by ICP-MS (2% HNO_3). For example, the dissolved silver concentrations after one and

284 two centrifugations were statistically different. For the targeted 4 μg/L solution, dissolved silver

285 concentrations decreased from 1.8 to 1.4 μg/L due to adsorption on the membrane (Figure S6).

286 The equilibrium was estimated to be achieved after five successive centrifugations. The selected

287 AgNPs concentration was that for which the dissolved Ag concentration at equilibrium was about

288 20 nM. Ultracentrifugation was also used as presented above during the accumulation

289 experiments in order to monitor the potential AgNPs oxidation/dissolution through time.

290 Exposure of the liposomes to silver nanoparticles was performed in a similar way to that

291 described for dissolved metals. Exposure solution 6 (Table 2) was prepared from the 9 mM

292 AgNPs solution. The liposomes, synthesized in the internal buffer solution (containing

293 thiosulfate), were exposed for 100 min. Every 10 min, a 5 min treatment with the Ambersep GT

294 74 resin (500 mg) was applied to liposomes exposed to nanoparticles. Analyses were performed

295 by ICP-MS as explained above.

296

297   Replication and Statistics

298   Every experiment was conducted at least twice ($n \geq 2$). Data were analysed for normality using

299   the Shapiro-Wilk test and for homogeneity of variance across treatments using Levene's test.

300   Student's t-tests were run to compare distributions with a size $n = 2$. One way ANOVA test was

301   applied to compare distributions with size $n > 2$. The effect of exposure time on the accumulation

302   of metals was evaluated using linear regressions. Non-linear regression (exponential rise to

303   maximum, Boullemant et al. (2009)) was used when it best fitted the data. Statistical analyses

304   were conducted at a 95% confidence interval ($\alpha = 0.05$) and graphs were created using SigmaPlot

305   12.5.

306

307   **Results**

308   Liposomes: mean diameter and size distribution

309   The Malvern Zetasizer Nano-ZS, used to determine the mean diameter and size distribution of the

310   liposomes, is an instrument based on dynamic light scattering (DLS). The size distribution most

311   frequently found in the literature is an intensity distribution (Z-average), calculated from the

312   instrument signal intensity. However, this distribution is highly affected by the presence of big

313   particles and is reliable only for monomodal samples with a polydispersity index (PDI) < 0.1. It

314   can be converted to a volume distribution (volume mean), which takes the particles' volume into

315   account (Malvern 2004).

316   The mean diameter and size distribution of the liposomes were determined immediately after their

317   synthesis, after their transfer to the pH 7.4 exposure solution, and once at the end of their

318   exposure to mercury (Table 3). The intensity and volume distributions were significantly different

319   after synthesis ($p < 0.05$); since the polydispersity index was higher than 0.1, the volume mean

320   was chosen as the reference value. The volume distributions after synthesis and after transfer to

321   the pH 7.4 buffer solution were also significantly different ($p < 0.05$). The size of the liposomes

322   tended to decrease after their transfer to the pH 7.4 buffer solution, from 173.0 ± 2.0 to $152.0 \pm$

323   6.0 nm in diameter. The reason for this decrease is unclear, given that the calculated ionic

324   strengths of the inner and outer solutions were similar at both pH values

325   Transfer to the pH 7.4 buffer solution

11

326   The liposomes (yellow fraction) eluted after 70 mL (Figure 2). The second fraction, in red, eluted

327   much later than the liposomes (elution volume = 265 mL). The background noise in absorbance at

328   432 nm was relatively low (around 0.06) and the results were reproducible: the elution volume of

329   the LUVs fraction (maximum absorbance between 70 and 75 mL) as well as the difference in

330   elution volume between fractions (around 150 mL) were similar for the three replicates.

331   Short term accumulation experiments

332   *Liposomes exposed to dissolved metals*

333   The accumulation of Ag^+ by liposomes (Figure 3a) had reached a plateau from the experiment

334   start (10 min) and no significant effect of time ($p > 0.05$) was observed on the accumulation of

335   Ag. Similar results were obtained for $HgCl_2^0$ (Figure 3b) and $Cd(DDC)_2^0$ (Figure 3f) ($p > 0.05$).

336   On the other hand, the accumulation of $AgS_2O_3^-$ as a function of time (Figure 3c) fitted a non-

337   linear regression as described by eq 6:

338    $$f = a(1 - e^{-bt}) \qquad\qquad\qquad\qquad\qquad\qquad (6)$$

339    $$[Ag]_L = [AgS_2O_3^-]^0 \cdot \frac{k_i}{k_e \cdot f_L} \cdot (1 - e^{-k_e \cdot f_L) \cdot t} \qquad\qquad\qquad\qquad (7)$$

340   where $[Ag]_L$ is the total Ag concentration in the liposomes (µmol Ag/g P), $[AgS_2O_3^-]^0$ the

341   concentration of the complex in the exposure solution (µmol/L), k_i the uptake constant (L/g

342   P·min), k_e the elimination constant (min^{-1}) and f_L the labile intracellular metal fraction (eq 7,

343   derived from Boullemant et al. (2009)).

344   A significant coefficient of determination (R^2=0.98, $p < 0.0001$, n=10) was obtained, indicating a

345   strong effect of time on the accumulation of silver complexed with thiosulfate (Figure 3c). A

346   similar result was obtained for $AgCl^0$ (Figure 3e) (R^2=0.90, $p < 0.0001$, n=10). No statistically

347   significant accumulation was observed for the experiment without thiosulfate in the internal

348   buffer solution (Figure 3d). In the absence of a trap in the internal buffer solution, silver can

349   adsorb to the surface of the liposomes but does not accumulate inside.

350   *Liposomes exposed to tritiated water*

351   Another experiment designed to test the liposomes' permeability was performed with tritiated

352   water. It was encapsulated inside the liposomes and passed through the steric exclusion

353   chromatography column. Figure 4 presents the radiometric results associated with the collected

354   fractions. The liposomes emerged after around 70 mL, as shown previously and a radioactivity of

355   only 6 cpm/mL, linked to the tritiated water concentration, was detected in the liposomes' main

356   fraction (70-80 mL).

357   *Liposomes exposed to silver nanoparticles*

358   We compared the ultrafiltered Ag concentrations (from 9 to 40 nM) after five successive

359   centrifugations of AgNPs solutions at different concentrations. We were then able to conclude

360   that the solution at 42 nM Ag_{total} was closest to the experimental conditions with dissolved silver

361   (20 nM $Ag_{dissolved}$, Figure S6, SI).

362   The oxidation of AgNPs as a function of time is presented in Figure 5. At time 0, only ~40% of

363   silver was in dissolved form. After about 20 min, a decrease in total Ag concentration was

364   observed in the solution (about 60%), presumably due to Ag adsorption. Silver was then present

365   mostly as dissolved (93%) and showed little variation over time, although a small statistically

366   significant increase was observed (one way ANOVA $p < 0.05$).

367   The liposome exposure experiment to nanosilver was repeated three times under the same

368   experimental conditions. The results were gathered in Figure 6. No statistically significant

369   increase (based on linear or non-linear regression analyses) was observed. Note that in the case

370   where the raw data (and not the averages) were collected on the same graph, the increase was

371   slightly significant ($p = 0.0224$) (Figure S7, SI).

372

Discussion

374   The biotic ligand model (BLM) is used to predict the bioavailability (and potential toxicity) of

375   metals in the aquatic environment towards aquatic organisms (Campbell et al. 2002). The BLM

376   predicts that, once a metal encounters the surface of a living cell, it may bind to surface sites

377   before being transported across the membrane. Typically, adsorption occurs very rapidly whereas

378   metal accumulation increases slowly over time (Campbell et al. 2002). In the context of our

379   study, if only metal adsorption on liposomes occurs, equilibrium should be reached rapidly. This

380   is the case for Ag^+ (cf. Figure 3a), which leads us to conclude that ionic silver did not diffuse

381   passively through the membrane of the liposomes but was only adsorbed at their surface.

382   Our results also suggest that $HgCl_2^0$ (Figure 3b) and $Cd(DDC)_2^0$ (Figure 3f) were also simply

383   adsorbed on the membrane of the liposomes, contrary to expectations. As mentioned in the

384   introduction, these two species are believed to be sufficiently hydrophobic ($K_{ow} = 3.3$, Mason et

385   al. (1996) and 270 ± 28 at pH 7, Boullemant et al. (2009), respectively) to pass through the lipid

386   membrane. Indeed, Mason et al. (1996) demonstrated that the coastal diatom *Thalassiosira*

387   *weissflogii* took up $HgCl_2^0$ by passive diffusion. Moreover, Bienvenue et al. (1984) and

388   Gutknecht (1981) studied the permeability of planar lipid bilayer membranes (PLMs), exposed to

389   the dichloromercury complex and demonstrated that it could cross the PLM by passive diffusion.

390   Finally, Boullemant et al. (2009) as well as Phinney and Bruland (1994) observed passive

391   diffusion of $Cd(DDC)_2^0$ through the cell membrane of three freshwater algae and a coastal

392   diatom, respectively.

393   Based on the solubility-diffusion model, the membrane should be permeant to water and small

394   neutral solutes (Finkelstein and Cass 1968), such as glycerol and urea (Paula et al. 1996), $HgCl_2^0$

395   or $Cd(DDC)_2^0$ (Finkelstein and Cass 1968). It is thus surprising that our model membrane does

396   not allow these species to pass. Several factors could have influenced these results. For example,

397   these species have relatively high molecular weights (272 g/mol for $HgCl_2^0$ and 408 g/mol for

398   $Cd(DDC)_2^0$). Cohen and Bangham (1972) showed that the diffusion of non-electrolytes (estimated

399   as the ratio of the measured permeability values to the oil/water partition coefficient) into

400   liposomes tended to decrease when the molecular weight increased. Note also that the water

401   permeability values for planar lipid membranes (PLMs) are on average one order of magnitude

402   higher than those for LUVs, suggesting that LUVs may be less permeable than PLMs (Deamer

403   and Bramhall 1986). For example, the water permeability coefficient for egg PC liposomes is 2.0

404   μm/s (Carruthers and Melchior 1983) against 40.2 μm/s for egg PC planar lipid bilayers

405   (Finkelstein and Cass 1967). Furthermore, Shimanouchi et al. (2011) noticed that the hydration of

406   the lipid bilayer depends on its curvature. In addition, metal interactions with membranes have

407   been shown to cause dehydration of liposomes, but only at mM concentrations (Kerek and

408   Prenner (2016), Klasczyk et al. (2010), Maity et al. (2016)). This parameter, regulating the

409   phospholipid headgroup mobility, varies as a function of liposome diameter and could then be

410   one of the determining factors influencing membrane permeability.

411   On the other hand, $AgS_2O_3^-$ and $AgCl^0$ were shown to be slowly internalised by liposomes, with

412   an apparent steady-state reached after 60 min of exposure (Figure 3c, e). Non-linear regressions

413   using (eq 4) allowed us to extract uptake constants k_i of 52.2 ± 4.4 mL/g P·min for $AgS_2O_3^-$ (24.2

414   nM) and 62.5 ± 19.2 mL/g P·min for $AgCl^0$ (24.5 nM). There is no significant difference between

415   both uptake constants (Student's t-test, p>0.05), therefore the liposomes seem to be as permeable

416   to $AgCl^0$ as to $AgS_2O_3^-$. Considering the absence of any apparent passive diffusion of the

417   lipophilic complexes $HgCl_2^0$ and $Cd(DDC)_2^0$, the uptake of $AgS_2O_3^-$ and $AgCl^0$ is puzzling. Fortin

14

and Campbell (2001) suggested that $AgS_2O_3^-$ could be transported into algal cells via sulfate/thiosulfate transport systems but to our knowledge the uptake of this complex has never been tested previously on artificial membranes. Some publications on lipid bilayers (Deamer and Bramhall (1986), Haydon and Hladky (1972); Sessa and Weissmann (1968)) suggest that the permeability of anions is significantly greater than that of cations (ex: 10^3 times higher for Cl^- than for Na^+ or K^+, Deamer and Bramhall (1986)). This could explain our results: the anionic complex $AgS_2O_3^-$ would pass through the membrane by passive diffusion, unlike the cation Ag^+. Note that this mechanism involves an exchange of anions between the inside of the liposomes and the external medium in order to respect solution electroneutrality. It may also be the case for $AgCl_2^-$, present in non-negligible proportions in the exposure solution 3 (14.5%, Table 2). With regards to the small $AgCl^0$ complex, the residual charges are important (with large dipoles), making it a very polar solute. We hypothesize that this complex can diffuse in a manner similar to anions or water molecules.

To determine if water molecules can diffuse through the lipid bilayer of our liposomes, we compared the initial and final ^3H activities after separation of the tritiated LUVs from the tritium solution. The initial ^3H activity was calculated as follows. The initial concentrated solution of tritiated water has an activity of 10 000 μCi/mL. During the liposome synthesis, this solution was diluted 45 times, leading to an activity of 222 μCi/mL or 8 222 000 Bq/mL. The internal volume of a 150-nm liposome is about $1.4 \cdot 10^{-15}$ mL and the number of liposomes per mL was $3.8 \cdot 10^{12}$ LUVs/mL (as determined by absorbance; see supporting information). Thus, the initial ^3H activity in the liposomes was estimated to be $5.5 \cdot 10^4$ Bq/mL of solution. Experimentally, only 0.25 Bq/mL was detected in the main liposomes fraction. The proportion of tritiated water recovered in the liposomes is thus equal to 0.00005 % of the initial activity. The tritiated water, initially used for liposomes synthesis, eluted after around 220 mL. Thus, the liposomes elution time (around 1 h, based on the elution speed) was sufficient for the encapsulated tritiated water to leave the LUVs, indicating that the liposomes are very permeable to water, as first demonstrated by Bangham et al. (1965). The water permeability of lipid membranes is crucial as it allows biological membranes to regulate their internal volume. The membranes exhibit a wide range of water permeability coefficients, depending on membrane lipid composition and structure, chain length and unsaturation, and cholesterol concentration (Deamer and Bramhall 1986). The water permeability of lipid bilayers is also higher for lipids in a liquid crystalline state ($T > T_{transition}$) than lipids in a gel state, which is the case in this study ($T > -2.5°C$) (Huster et al. 1997).

15

450   When AgNPs are suspended in our exposure solutions, changes were observed (Figure 5). The

451   observed trend could be due to the oxidation of AgNPs, increasing the proportion of dissolved Ag

452   and the subsequent adsorption of Ag on the container walls. Liposomes exposed to a low

453   concentration of silver nanoparticles showed no significant increase in Ag accumulation (Figure

454   6). This is consistent with the fact that no studies have shown that silver nanoparticles can pass

455   through the phospholipid membrane by passive diffusion. Le Bihan et al. (2009) studied the

456   invagination of silica nanoparticles by liposomes. They indicated that this process was very rapid

457   and that it would have been difficult to analyze it without using a method to slow it down. Thus,

458   they covered silica nanoparticles with gold nanoparticles (positively charged, 10 nm) which made

459   it possible to slow down the liposomes spreading on the silica surface. They were then able to

460   observe the intermediate steps of the engulfment process by cryo-TEM. If an invagination of

461   AgNPs-PVPs by liposomes had occurred, its observation would not have been possible under our

462   experimental conditions. It would have been possible to apply a treatment similar to that set up by

463   Le Bihan et al. (2009) in order to slow down the process and to observe or not this invagination,

464   within the 20 to 30 min where silver nanoparticles are still present and relatively intact in solution

465   (Figure 5). Nevertheless, based on Le Bihan et al. (2009), our AgNPs with a size less than or

466   equal to 5 nm would not possess sufficient adhesion strength to cause invagination and could only

467   adsorb to the surface of the liposomes. Moreover, considering the small amounts of silver found

468   associated with the liposomes (on average 38.3 μmol Ag / g P, corrected for the residual amount

469   of Ag), we can hypothesize that the invagination of silver nanoparticles is unlikely and that

470   AgNPs only adsorbed to the surface of the liposomes, as has been shown by Wang et al. (2016).

471

Conclusion

473   The objective of this study was to test if nanoparticulate silver could cross a lipid bilayer. To do

474   this we used 150-nm liposomes made of phosphatidylcholine. Because nanoparticulate silver

475   always release dissolved ions, we first had to characterize the passive diffusion of dissolved

476   species of Ag(I). This was done by performing short term experiments under different conditions

477   where Ag^+, $AgS_2O_3^-$ or $AgCl^0$ were the dominant species. The permeability of liposomes was also

478   tested with $HgCl_2^0$, $Cd(DDC)_2^0$ and ^3H_2O. Our liposomes proved to be impermeable to ionic and

479   nanoparticulate silver. Considering that we used nanoparticles among the smallest available on

480   the market with the most neutral coating which would favor its passive diffusion across a lipid

481   bilayer, our results suggest that nanoparticles cannot diffuse through a bilipid membrane.

482 On the other hand, it appeared that our artificial lipid bilayer could be more permeable to anions

483 such as $AgS_2O_3^-$ than to cations. However, this is not an inherent property of biological

484 membranes of living organisms. Although liposomes have often been used to study the

485 interaction between contaminants and biological membranes, there remains a large gap between

486 LUVs and living cells. Indeed, the hydrophobic complexes $HgCl_2^0$ and $Cd(DDC)_2^0$ did not pass

487 through the phospholipid bilayer of our liposomes, contrary to what have been previously

488 demonstrated for biological membranes. Therefore an extrapolation of the liposomes results to

489 toxicological studies must be made with caution.

490

495   **References**

496

497   Bangham AD, Standish MM, Watkins JC (1965) Diffusion of univalent ions across the lamellae

498   of swollen phospholipids. J Mol Biol 13:238-252 doi:10.1016/S0022-2836(65)80093-6

499   Berger N, Sachse A, Bender J, Schubert R, Brandl M (2001) Filter extrusion of liposomes using

500   different devices: comparison of liposome size, encapsulation efficiency, and process

501   characteristics. Int J Pharm 223:55-68 doi:10.1016/S0378-5173(01)00721-9

502   Bienvenue E, Boudou A, Desmazes JP, Gavach C, Georgescauld D, Sandeaux J, Sandeaux R,

503   Seta P (1984) Transport of mercury compounds across bimolecular lipid membranes:

504   effect of lipid composition, pH and chloride concentration. Chem Biol Interact 48:91-101

505   doi:10.1016/0009-2797(84)90009-7

506   Blaser SA, Scheringer M, MacLeod M, Hungerbuhler K (2008) Estimation of cumulative aquatic

507   exposure and risk due to silver: Contribution of nano-functionalized plastics and textiles.

508   Sci Total Environ 390:396-409 doi:10.1016/j.scitotenv.2007.10.010

509   Boullemant A, Lavoie M, Fortin C, Campbell PGC (2009) Uptake of Hydrophobic Metal

510   Complexes by Three Freshwater Algae: Unexpected Influence of pH. Environ Sci

511   Technol 43:3308-3314 doi:10.1021/es802832u

512   Campbell PGC (1995) Interactions between trace metals and aquatic organisms: a critique of the

513   free-ion activity model. In: Tessier A, Turner DR (eds) Metal speciation and

514   bioavailability in aquatic systems. John Wiley & Sons Ltd, pp 45-102

515   Campbell PGC, Errécalde O, Fortin C, Hiriart-Baer VP, Vigneault B (2002) Metal bioavailability

516   to phytoplankton—applicability of the biotic ligand model. Comp Biochem Physiol C:

517   Pharmacol Toxicol 133:189-206 doi:10.1016/S1532-0456(02)00104-7

518   Carrozzino JM, Khaledi MG (2005) pH effects on drug interactions with lipid bilayers by

519   liposome electrokinetic chromatography. J Chromatogr A 1079:307-316

520   doi:10.1016/j.chroma.2005.04.008

521   Carruthers A, Melchior DL (1983) Studies of the relationship between bilayer and water

522   permeability and bilayer physical state. Biochem 22:5797-5807 doi:10.1021/bi00294a018

523   Castile JD, Taylor KMG (1999) Factors affecting the size distribution of liposomes produced by

524   freeze–thaw extrusion. Int J Pharm 188:87-95 doi:10.1016/S0378-5173(99)00207-0

525   Cohen BE, Bangham AD (1972) Diffusion of small nonelectrolytes across liposomes membranes.

526   Nature 236:173-& doi:10.1038/236173a0

527   Deamer DW, Bramhall J (1986) Permeability of lipid bilayers to water and ionic solutes. Chem

528   Phys Lipids 40:167-188 doi:10.1016/0009-3084(86)90069-1

18

529   Ducat E, Brion M, Lecomte F, Evrard B, Piel G (2010) The experimental design as practical
530   approach to develop and optimize a formulation of peptide-loaded liposomes. AAPS
531   PharmSciTech 11:966-975 doi:10.1208/s12249-010-9463-3

532   Enoch HG, Strittmatter P (1979) Formation and properties of 1000-A-diameter, single-bilayer
533   phospholipid vesicles. Proc Nat Acad Sci USA 76:145-149 doi:10.1073/pnas.76.1.145

534   Finkelstein A, Cass A (1967) Effect of cholesterol on the water permeability of thin lipid
535   membranes. Nature 216:717-718 doi:10.1038/216717a0

536   Finkelstein A, Cass A (1968) Permeability and electrical properties of thin lipid membranes. J
537   Gen Physiol 52:145-172 doi:10.1085/jgp.52.1.145

538   Fortin C, Campbell PGC (2000) Silver uptake by the green alga *Chlamydomonas reinhardtii* in
539   relation to chemical speciation: Influence of chloride. Environ Toxicol Chem 19:2769-
540   2778 doi:10.1002/etc.5620191123

541   Fortin C, Campbell PGC (2001) Thiosulfate enhances silver uptake by a green alga: Role of anion
542   transporters in metal uptake. Environ Sci Technol 35:2214-2218 doi:10.1021/es0017965

543   Gottschalk F, Sonderer T, Scholz RW, Nowack B (2009) Modeled environmental concentrations
544   of engineered nanomaterials (TiO$_2$, ZnO, Ag, CNT, fullerenes) for different regions.
545   Environ Sci Technol 43:9216-9222 doi:10.1021/es9015553

546   Gutknecht J (1981) Inorganic mercury (Hg^{2+}) transport through lipid bilayer membranes. J
547   Membr Biol 61:61-66 doi:10.1007/bf01870753

548   Haydon DA, Hladky SB (1972) Ion transport across thin lipid-membranes - critical discussion of
549   mechanisms in selected systems. Q Rev Biophys 5:187-282
550   doi:10.1017/S0033583500000883

551   Huster D, Jin AJ, Arnold K, Gawrisch K (1997) Water permeability of polyunsaturated lipid
552   membranes measured by O-17 NMR. Biophys J 73:855-864 doi:10.1016/S0006-
553   3495(97)78118-9

554   Kerek EM, Prenner EJ (2016) Inorganic cadmium affects the fluidity and size of phospholipid
555   based liposomes. Biochimica et Biophysica Acta (BBA) - Biomembranes 1858:3169-
556   3181 doi:10.1016/j.bbamem.2016.10.005

557   Klasczyk B, Knecht V, Lipowsky R, Dimova R (2010) Interactions of Alkali Metal Chlorides
558   with Phosphatidylcholine Vesicles. Langmuir 26:18951-18958 doi:10.1021/la103631y

559   Koynova R, Caffrey M (1998) Phases and phase transitions of the phosphatidylcholines. Biochim
560   Biophys Acta, Biomembr 1376:91-145 doi:10.1016/s0304-4157(98)00006-9

561   Le Bihan O et al. (2009) Cryo-electron tomography of nanoparticle transmigration into liposome.
562   J Struct Biol 168:419-425 doi:10.1016/j.jsb.2009.07.006

563 Levard C, Hotze EM, Lowry GV, Brown GE, Jr. (2012) Environmental transformations of silver
564   nanoparticles: impact on stability and toxicity. Environ Sci Technol 46:6900-6914
565   doi:10.1021/es2037405

566 Maity P, Saha B, Kumar GS, Karmakar S (2016) Binding of monovalent alkali metal ions with
567   negatively charged phospholipid membranes. Biochimica Et Biophysica Acta-
568   Biomembranes 1858:706-714 doi:10.1016/j.bbamem.2016.01.012

569 Malvern (2004) Zetasizer nano series user manual - MAN0317 Issue 2.1. Malvern Instruments
570   Ltd.

571 Martell AE, Smith RM, Motekaitis RJ (2004) NIST critically selected stability constants of metal
572   complexes v. 8.0. National Institute of Standards and Technology, Gaithersburg, MD,
573   USA

574 Mason RP, Reinfelder JR, Morel FMM (1996) Uptake, toxicity, and trophic transfer of mercury
575   in a coastal diatom. Environ Sci Technol 30:1835-1845 doi:10.1021/es950373d

576 MDDELCC (2016) Suivi de la qualité des rivières et petits cours d'eau.
577   http://www.mddelcc.gouv.qc.ca/eau/eco_aqua/rivieres/annexes.htm#ph. Accessed 27
578   October 2016.

579 Miao AJ, Luo ZP, Chen CS, Chin WC, Santschi PH, Quigg A (2010) Intracellular uptake: A
580   possible mechanism for silver engineered nanoparticle toxicity to a freshwater alga
581   *Ochromonas danica*. PLoS One 5:e15196 doi:e1519610.1371/journal.pone.0015196

582 Moghadam BY, Hou WC, Corredor C, Westerhoff P, Posner JD (2012) Role of nanoparticle
583   surface functionality in the disruption of model cell membranes. Langmuir 28:16318-
584   16326 doi:10.1021/la302654s

585 Nyman CJ, Salazar T (1961) Complex ion formation of mercury(II) and thiosulfate ion. Anal
586   Chem 33:1467-1469 doi:10.1021/ac60179a005

587 Paula S, Volkov AG, VanHoek AN, Haines TH, Deamer DW (1996) Permeation of protons,
588   potassium ions, and small polar molecules through phospholipid bilayers as a function of
589   membrane thickness. Biophys J 70:339-348 doi:10.1016/S0006-3495(96)79575-9

590 Phinney JT, Bruland KW (1994) Uptake of lipophilic organic Cu, Cd, and Pb complexes in the
591   coastal diatom *Thalassiosira weissflogii*. Environ Sci Technol 28:1781-1790
592   doi:10.1021/es00060a006

593 Reinfelder JR, Chang SI (1999) Speciation and microalgal bioavailability of inorganic silver.
594   Environ Sci Technol 33:1860-1863 doi:10.1021/es980896w

595   Rusciano G, De Luca AC, Pesce G, Sasso A (2009) On the interaction of nano-sized organic
596   carbon particles with model lipid membranes. Carbon 47:2950-2957
597   doi:10.1016/j.carbon.2009.06.042
598   Schecher WD, McAvoy D (2001) MINEQL+: A Chemical Equilibrium Modeling System. 4.62
599   edn. Environmental Research Software, Hallowell, ME, USA
600   Sessa G, Weissmann G (1968) Phospholipid sherules (liposomes) as a model for biological
601   membranes. J Lipid Res 9:310-318
602   Shimanouchi T, Sasaki M, Hiroiwa A, Yoshimoto N, Miyagawa K, Umakoshi H, Kuboi R (2011)
603   Relationship between the mobility of phosphocholine headgroups of liposomes and the
604   hydrophobicity at the membrane interface: A characterization with spectrophotometric
605   measurements. Colloid Surf B-Biointerfaces 88:221-230
606   doi:10.1016/j.colsurfb.2011.06.036
607   Treuel L, Jiang XE, Nienhaus GU (2013) New views on cellular uptake and trafficking of
608   manufactured nanoparticles. J R Soc Interface 10:14 doi:10.1098/rsif.2012.0939
609   Turner A, Mawji E (2004) Hydrophobicity and octanol-water partitioning of trace metals in
610   natural waters. Environ Sci Technol 38:3081-3091
611   Villarreal MR (2007) Cross section of a liposome via wikimedia.org (public property).
612   Wang Q, Lim M, Liu X, Wang Z, Chen KL (2016) Influence of solution chemistry and soft
613   protein corona on the interactions of silver nanoparticles with model biological
614   membranes. Environ Sci Technol 50:2301-2309 doi:10.1021/acs.est.5b04694

615

Table 1.Composition of the buffer solutions (ionic strength and speciation calculated using MINEQL+ v.4.6)

Buffer solutions	Composition	pH	I (mM)	Speciation
Internal buffer solution	Phenol red sodium salt 6.0 mM; MES acid buffer 5.0 mM; $Na_2S_2O_3$ 1.33 mM; NaOH 2.4 mM; KNO_3 15.9 mM.	6.0	25.0	99.2 % $Ag(S_2O_3)_2^{3-}$ 65.4 % $Hg(S_2O_3)_2^{2-}$ 34.6 % $Hg(S_2O_3)_3^{4-}$
Internal buffer solution (w/o trap)	Phenol red sodium salt 6.0 mM; MES acid buffer 5.0 mM; NaOH 2.4 mM; KNO_3 23.1 mM.	6.0	25.0	98.7 % Ag^+ 99.9% Hg^{2+} 97% Cd^{2+}
Internal buffer solution (EDTA)	Phenol red sodium salt 6.0 mM; MES acid buffer 5.0 mM; EDTA 2.0 mM; NaOH 2.4 mM; KNO_3 13.3 mM.	6.0	25.0	99.9 $Cd(EDTA)^{2-}$
Exposure buffer solution	MOPS acid buffer 7.5 mM ; NaOH 5.6 mM ; KNO_3 19.9 mM	7.4	25.0	/

Table 2.Composition of the exposure solutions, after dilution with the liposome dispersion (ionic strength and speciation calculated using MINEQL+ v.4.6).

	Composition	pH	I (mM)	Speciation
Exposure solution 1	MOPS acid buffer 7.2 mM; NaOH 14.7 mM; $AgNO_3$ 30 nM; KNO_3 15.4 mM	7.4	25.0	Ag^+ 99.1 %
Exposure solution 2	MOPS acid buffer 7.0 mM; NaOH 14.7 mM; $AgNO_3$ 30 nM; $Na_2S_2O_3$ 173.2 nM; KNO_3 15.5 mM	7.4	25.0	$AgS_2O_3^-$ 96.9 %; $Ag(S_2O_3)_2^{3-}$ 1.2 %; Ag^+ 1.9 %
Exposure solution 3	MOPS acid buffer 7.0 mM; NaOH 14.8 mM; NaCl 2.5 mM; $AgNO_3$ 30 nM ;KNO_3 12.9 mM	7.4	25.0	$AgCl^0$ 67.2 %; $AgCl_2^-$ 14.5 %; Ag^+ 18.1 %
Exposure solution 4	MOPS acid buffer 6.8 mM; NaCl 4.9 mM; NaOH 5.2 mM; $HgCl_2$ 146.9 nM; KNO_3 15.4 mM	7.4	25.0	$HgCl_2^0$ 42.7 %; $HgClOH^0$ 45.4 %; $HgCl_3^-$ 2.1 %; $Hg(OH)_2^0$ 9.8 %
Exposure solution 5	MOPS acid buffer 6 mM; Na-DDC 700 nM; NaOH 4.8 mM; $Cd(NO_3)_2$ 150 nM; KNO_3 20.8 mM	7.4	25.0	$Cd(DDC)_2^0$ 99.9 %
Exposure solution 6	MOPS acid buffer 7.5 mM; NaOH 5.6 mM; AgNPs-PVP 72.5 nM; KNO_3 19.8 mM	7.4	25.0	Ag^+ 98.9 % (for dissolved silver, disregarding the presence of AgNPs)

Table 3. Size distributions of the liposomes, determined by dynamic light scattering, after their synthesis, their transfer to the pH 7.4 buffer solution and their exposure to silver. Mean ± standard deviation.

	After synthesis (n=4) PdI* = 0.125 ± 0.02	After transfer to the pH 7.4 buffer solution (n=6) PdI* = 0.112 ± 0.005	After exposure to mercury (n=1) PdI* = 0.160
Z-average diameter	161.8 ± 1.6 nm^a	151.2 ± 5.6 nm^c	142.5 nm
Volume mean diameter	173.0 ± 2.0 nm^b	152.0 ± 6.0 nm^c	144.1 nm

*PdI : Polydispersity Index
Values with different lower case letters are significantly different ($p < 0.05$).
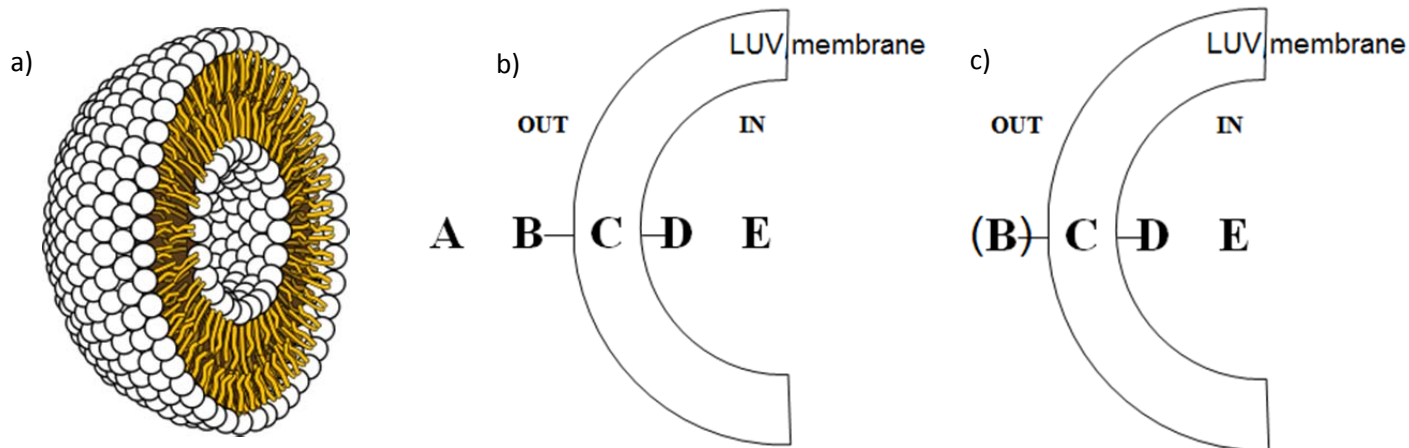
Figure 1. Cross section of a liposome (Villarreal 2007) a) and potential metal localizations after interaction with the liposomes: A. in the bulk solution, B. adsorbed at the surface of the liposomes, C. inside the lipid bilayer, D. adsorbed at the surface of the liposome in the inner solution, E. in the internal solution before b) and after c) treatment with Ambersep GT74 resin. (B) in Figure 1c) : The Ambersep GT74 resin may not be 100% efficient in removing metal adsorbed at the surface of the liposomes.
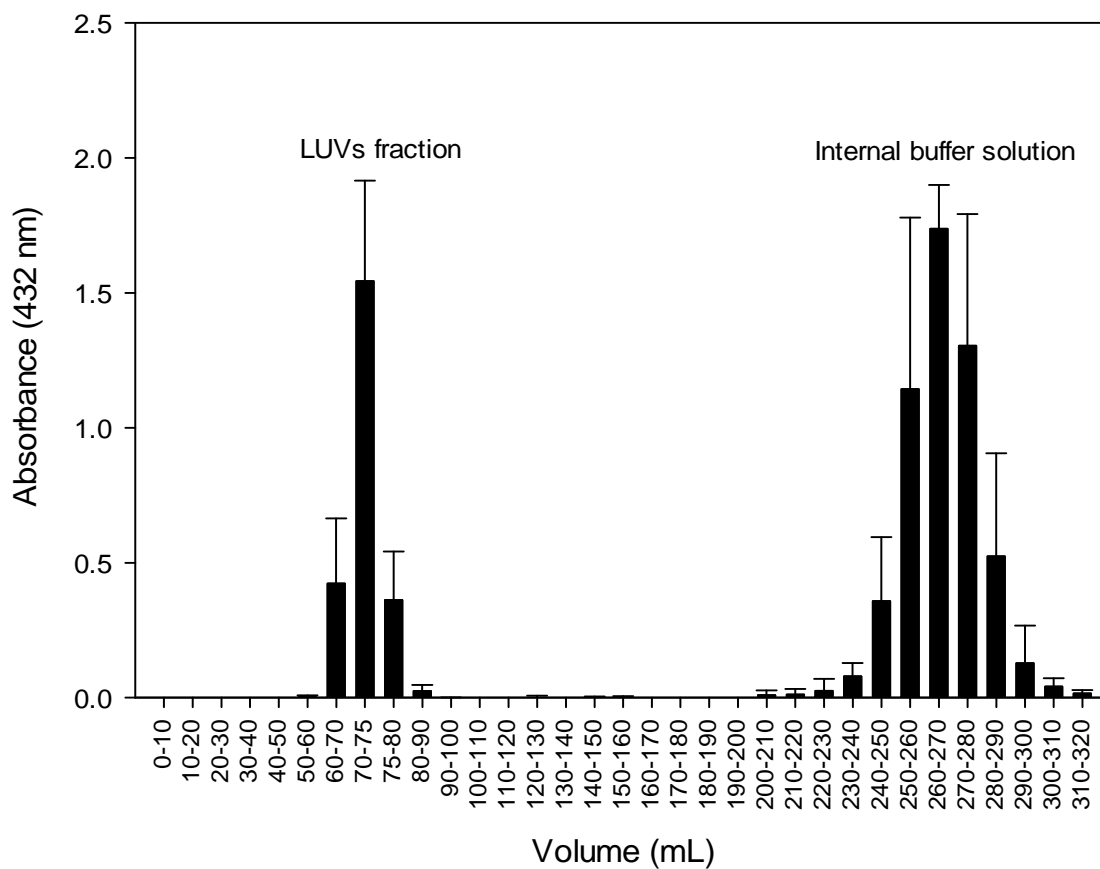
Figure 2. Presence of liposomes as determined by absorbance at 432 nm after the transfer of the liposomes to the pH 7.4 buffer solution. Liposomes were separated from the buffer solution by size exclusion chromatography. Eluant was collected in 10 mL fractions. Mean ± standard deviation (n=3).
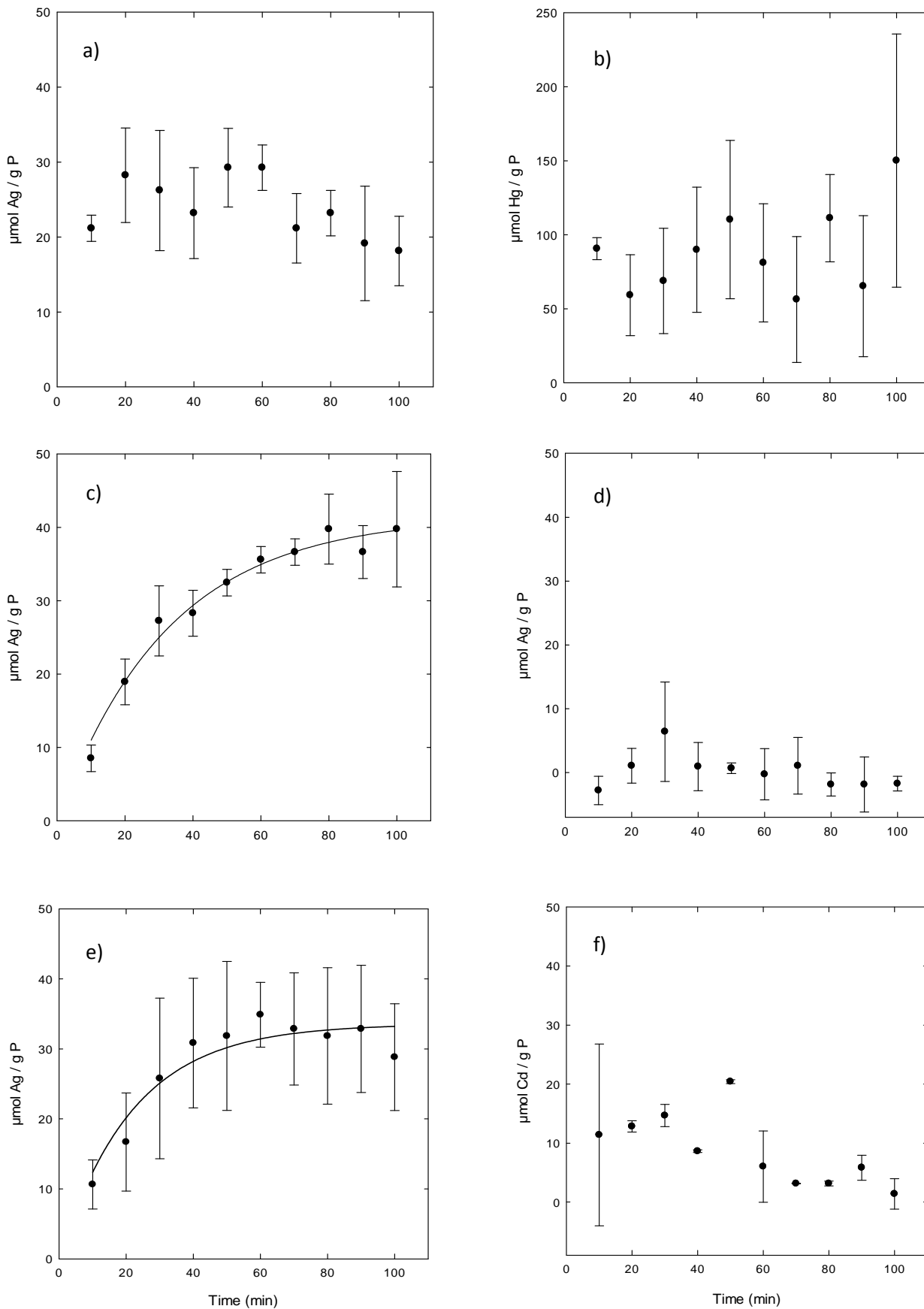
Figure 3. Accumulation of a) Ag^+ b) $HgCl_2^0$ c) $AgS_2O_3^-$ d) $AgS_2O_3^-$ (without internal metal trap) e) $AgCl^0$ f) $Cd(DDC)_2^0$ by liposomes over time, corrected for the residual quantity of dissolved metal. Mean ± standard deviation (n=3). No statistically significant increase observed for a) b) d) and f) (non-linear regression, p > 0.05).
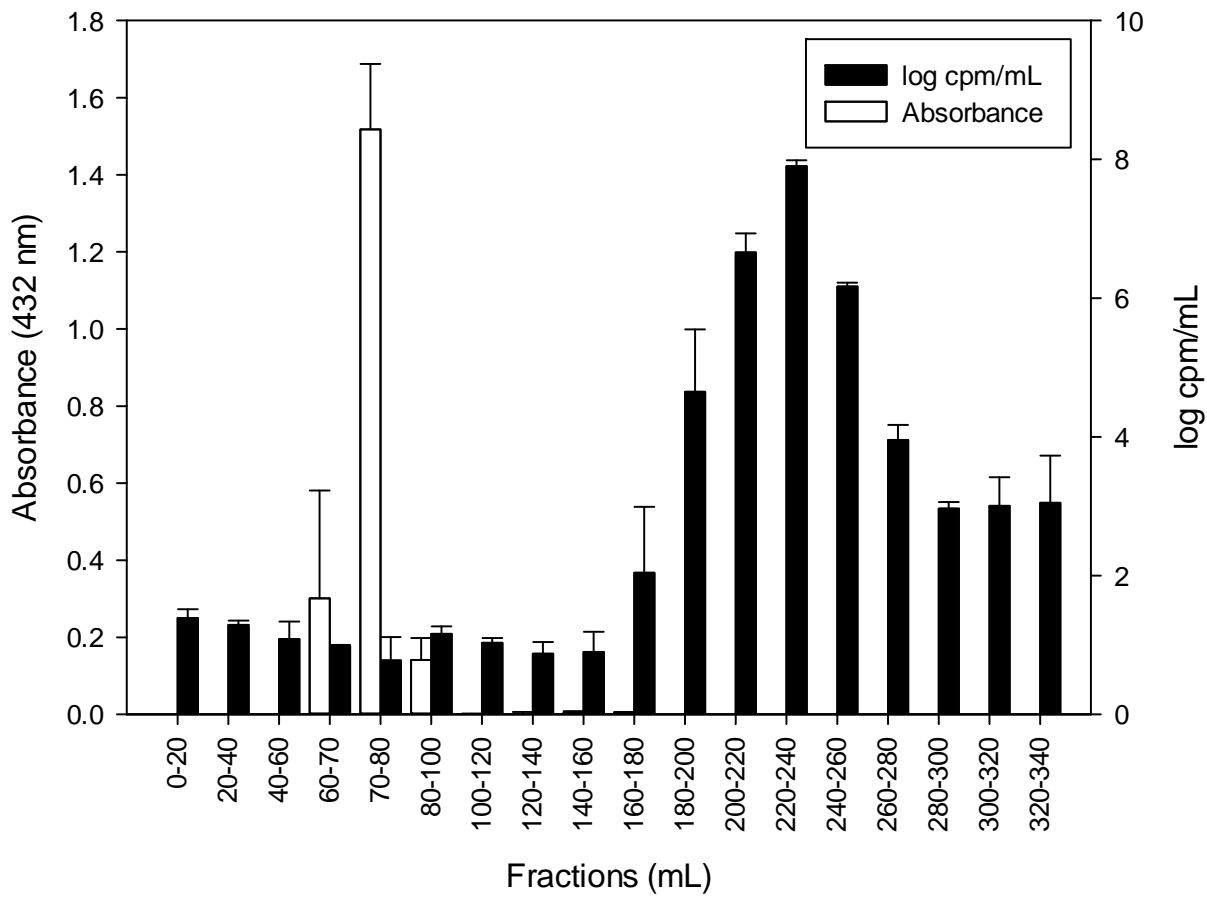
Figure 4. Presence of liposomes as determined by absorbance at 432 nm and tritium activity determined in each fraction collected from a steric exclusion column. Mean ± standard deviation (n=2).
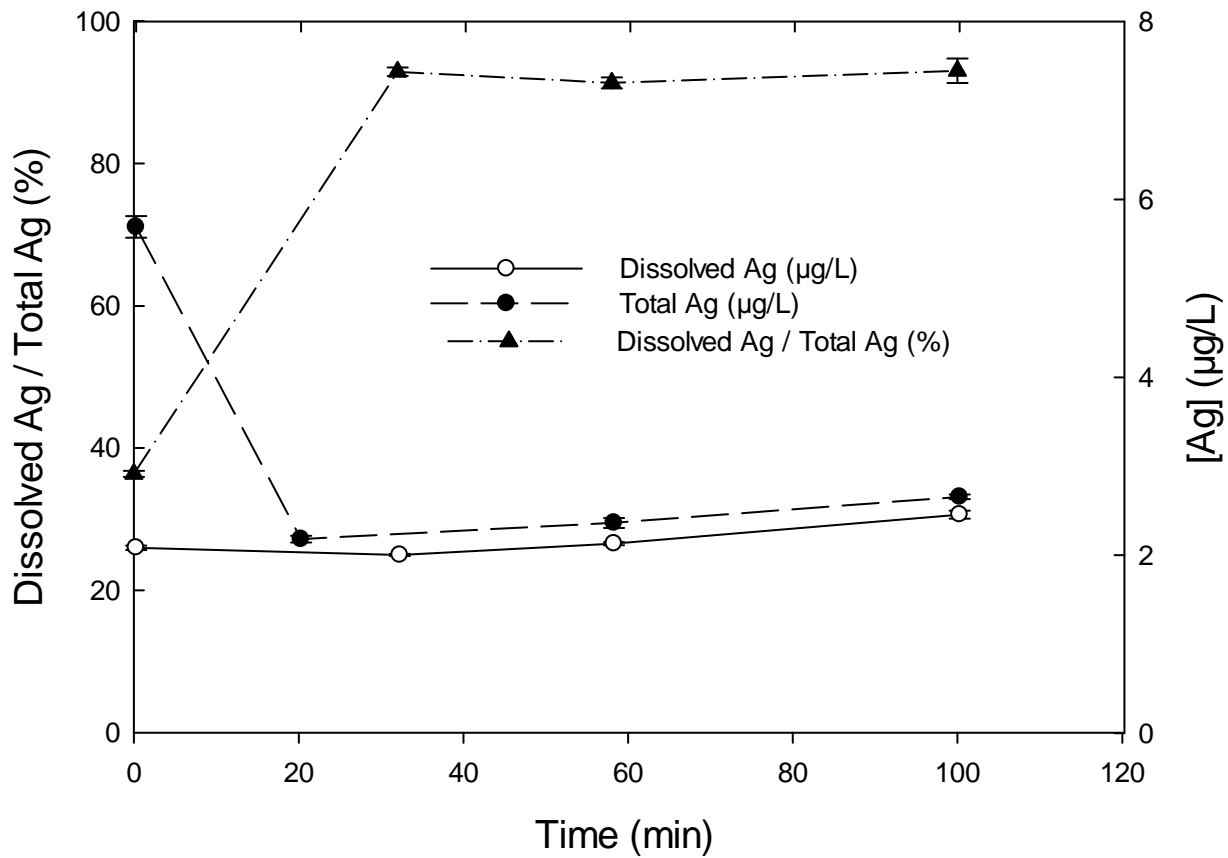
Figure 5. Oxidation of AgNPs as a function of time in exposure solution 6 (MOPS acid buffer 7.5 mM ; NaOH 5.6 mM ; AgNPs-PVP 72.5 nM ; KNO_3 19.8 mM) and in the presence of liposomes. Mean ± standard deviation (n = 3). A small statistically significant increase observed for dissolved silver (one way ANOVA p <0.05).
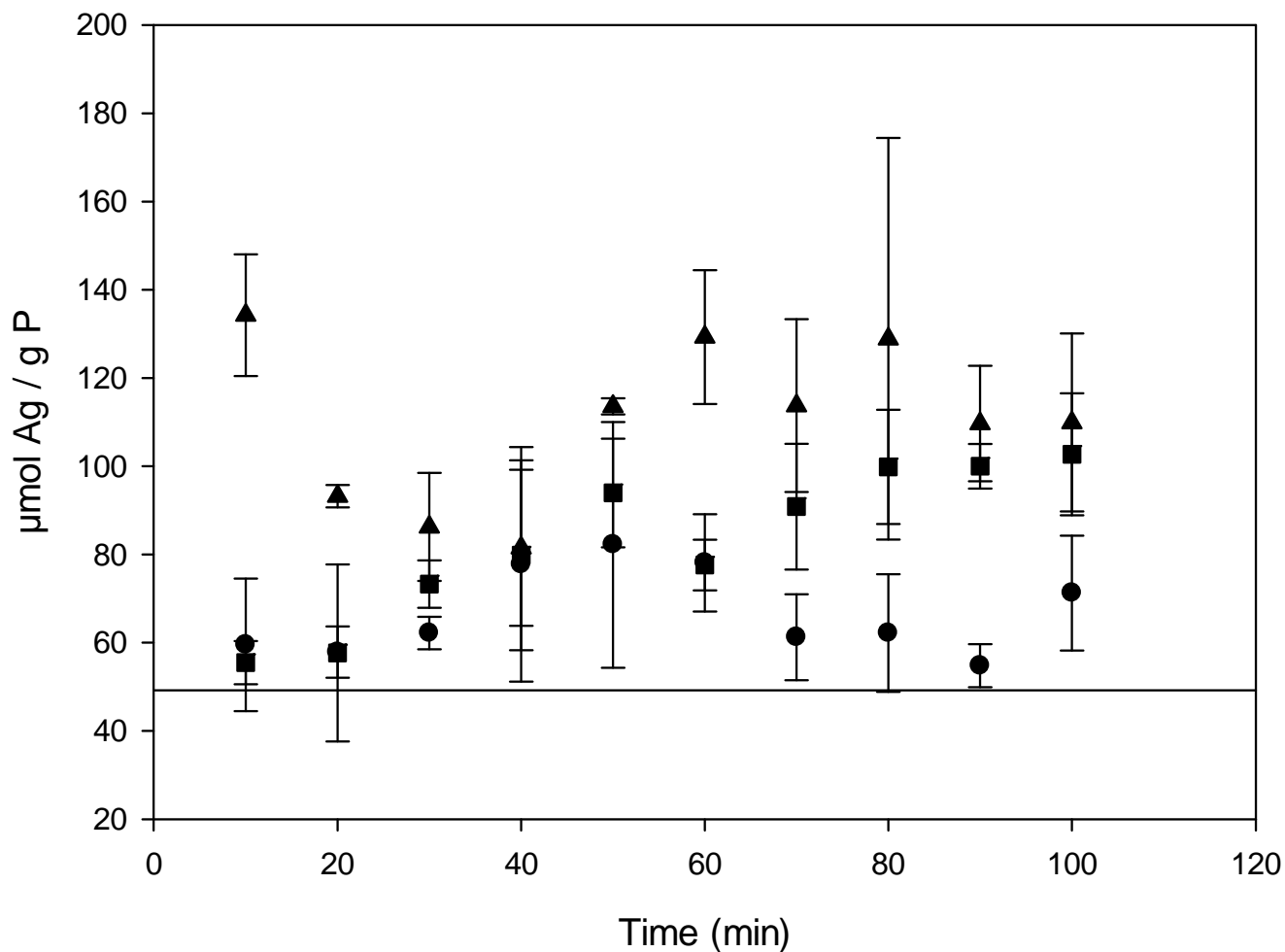
Figure 6. Accumulation of Ag by liposomes over time when exposed to AgNPs. The horizontal line corresponds to the residual quantity of dissolved metal. Mean ± standard deviation (n=3). Each set of symbols corresponds to one experiment. No statistically significant increase observed (linear and non-linear regression : exponential rise to maximum, Boullemant et al. (2009)).